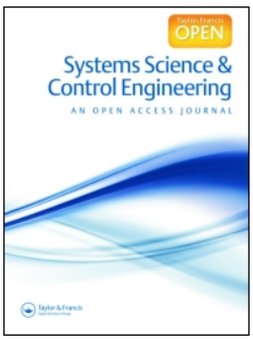

Systems Science & Control Engineering

An Open Access Journal

ISSN: (Print) 2164-2583 (Online) Journal homepage: https://www.tandfonline.com/loi/tssc20

Base-scale entropy and energy analysis of flow characteristics of the two-phase flow

Chunling Fan, Qihua Fan & Haojie Li

To cite this article: Chunling Fan, Qihua Fan & Haojie Li (2018) Base-scale entropy and energy analysis of flow characteristics of the two-phase flow, Systems Science & Control Engineering, 6:3, 262-269, DOI: 10.1080/21642583.2018.1547884

To link to this article: https://doi.org/10.1080/21642583.2018.1547884

Published online: 29 Nov 2018.

SYSTEMS SCIENCE & CONTROL ENGINEERING: AN OPEN ACCESS JOURNAL
2018, VOL. 6, NO. 3, 262–269
https://doi.org/10.1080/21642583.2018.1547884

Taylor & Francis
Taylor & Francis Group

Base-scale entropy and energy analysis of flow characteristics of the two-phase flow

Chunling Fan, Qihua Fan and Haojie Li

College of Automation and Electronic Engineering, Qingdao University of Science and Technology, Qingdao, People's Republic of China

ABSTRACT

In this paper, the base-scale entropy and root mean square energy analysis method are combined to present a simple and quick strategy to extract the features of the gas–liquid two-phase flow and to characterize the different flow patterns. In order to verify the effectiveness of the extracted features, we calculate their separability measure values. The experimental results show that the combined strategy proposed in this paper can not only distinguish the different flow patterns but also complement each other.

ARTICLE HISTORY
Received 26 June 2018
Accepted 10 November 2018

KEYWORDS
Gas–liquid two-phase flow; base-scale entropy; energy analysis; root mean square; separability measure; flow characteristics

1. Introduction

The gas–liquid two-phase flow (Li, 1991; Tan & Dong, 2013) is a typical nonlinear system, which is widely existed in industrial fields. The flow pattern, which is the distribution of the flowing medium between two-phase flow phases, plays a very important role in the study of two-phase flow parameters. It can greatly affect the two-phase flow pressure gradient and heat and mass transfer rate and other characteristics, and also the measurement accuracy of flow process parameters and other relevant characteristics. Although various methods have been applied to the research of the two-phase flow patterns, the complexity of flow dynamics needs to be further investigated.

In recent years, the concept and research method of nonlinear analysis is widely applied in the study of chaotic signals, one of the most representative methods is the entropy method (Li, Li, & Zhang, 2017; Liu & Shang, 2018). Entropy method with the advantages of simplicity, extremely fast calculation and anti-noise characteristics is convenient for detecting useful information of time series. Li, Zhou, Ren, and Yang (2012) used the symbolic dynamics Shannon entropy method to study the conductance signals of the gas–liquid two-phase flow, and the results indicated that it is an effective method for the analysis of two-phase flow conductance signals, different flow patterns can be distinguished and the evolution characteristics of different flow patterns can be identified. Zhou, Yin, and Ding (2016) used a multi-scale entropy analysis to study time series of pressure difference signals of the gas–liquid two-phase flow in the 7×7 rod bundled channel under 104 different flow conditions. Results showed that the change rate of multi-scale entropy in small scales (no more than 8) can accurately distinguish four flow regimes in the rod bundled channel, whereas the trending of large scale sample entropy could disclose dynamic characteristics of each flow regime. Jin et al (Fan, Jin, Chen, Dou, & Gao, 2015) used the multi-scale complexity entropy causality plane (MS-CECP) method to investigate typical chaotic time series and to process the conductance fluctuating signals of three typical gas–liquid flow patterns. The results indicated that the single-scale CECP can discriminate the different flow patterns linearly, and MS-CECP can describe the continuous information loss of flow structures with the increase of scale, which reflects the dynamical stability and complexity of gas–liquid two-phase flow system.

The entropic methods discussed above can be used to characterize two-phase flow patterns, but they have a higher demand on the amount of data points. Recently, Li et al. (Li & Liu, 2012; Liu, Yao, Ning, Ni, & Wang, 2013) presented the basic-scale entropy (BE) method which can be used to distinguish different heart rate variability signals clearly. This method needs less data and calculates quickly, also it has the great anti-interference ability. In addition, the energy analysis method has been broadly utilized for system performance evaluation. Hüseyin Göksu (2018) used the log energy entropy with wavelet packet decomposition method to analyse BCI-oriented EEG, and the experimental results demonstrated

CONTACT Chunling Fan peakfan@163.com

that this method was effective. Hu, Mu, and Xiao (2008) extracted the features of different EEG signals by the energy entropy method, and classified the EEG signals based on the features. The results showed that classification accuracy can exceed 90%. The root mean square (RMS) method, as a simple energy analysis method, has been broadly utilized for research of the bearing fault diagnosis (Wu, Wu, Wu, & Wang, 2013).

In this paper, we use the basic-scale entropy and energy analysis method to analyse the characteristics of flow patterns and to achieve a good result. The method proposed in this paper needs less data and calculates quickly and can characterize the complexity of different patterns for gas–liquid two-phase flow significantly.

2. Base-scale entropy

2.1. The basic-scale entropy theory

For a given time series y of N points $\{y(i) : 1 \le i \le N\}$, we choose continuous m data points to construct an m-dimensional space

$$Y(i) = [y(i), y(i+1), \cdots, y(i+(m-1))] \tag{1}$$

where m is the embedding dimension. There are $N-m+1$ m-dimensional vectors. For each m-dimensional vector, the base scale $\lambda(i)$ is defined as the root mean square of differences between every two continuous data points in the m-dimensional vector, and the equation is

$$\lambda(i) = \sqrt{\frac{\sum_{j=1}^{m-1} [y(i+j) - y(i+j-1)]^2}{m-1}}, \quad i = 1, 2 \cdots, N-m+1. \tag{2}$$

According to $\lambda(i)$, every m-dimensional vector can be transformed into a symbolic sequence $S_i(Y(i)) = \{s(i), s(i+1), \cdots, s(i+m-1)\}, s(i) \in A\ (A = 0, 1, 2, 3)$. The set A is just for count probability, and its values have no practical meanings.

$$S_i(Y(i)) = \begin{cases} 0, & y_{i+k} \le \bar{y}_i - \alpha\lambda(i) \\ 1, & \bar{y}_i - \alpha\lambda(i) < y_{i+k} \le \bar{y}_i \\ 2, & \bar{y}_i < y_{i+k} \le \bar{y}_i + \alpha\lambda(i) \\ 3, & y_{i+k} > \bar{y}_i + \alpha\lambda(i) \end{cases} \tag{3}$$

where $i = 1, 2, 3 \cdots, N-m+1, k = 0, 1, 2, \cdots, m-1$, $\bar{y}_i$ is the mean of the ith m-dimensional vector, $\lambda(i)$ is the base scale and is also the standard for dividing symbols, and α is a special parameter. If α is too large, then the detailed information will be lost, and if α is too small, then the dynamic information of time series cannot be caught.

To calculate the value of the base-scale entropy, we study the distributing probability $p(S_i)$ about the symbolic sequence S_i of the ith m-dimensional vector. The symbolic sequence S_i is made up of four symbols (0, 1, 2, 3), which has 4^m different type states π. For $N-m+1$ m-dimensional vectors, the relative probability is given as

$$p(\pi) = \frac{\#\{t | (y_t, \cdots, y_{t+m-1}) \text{ has type } \pi\}}{N-m+1} \tag{4}$$

where $1 \le t \le N-m+1$, and # means the number having different type states, and π means different type states.

The base-scale entropy (Fan, Haojie, & Yinghui, 2015; Yan & Zhao, 2011) of m-dimensional vector is defined as

$$H(m) = -\sum p(\pi) \log_2 p(\pi) \tag{5}$$

where $3 \le m \le 7, N \ge 4^m$.

$H(m)$ describes the information contained in m consecutive values of the time series. The larger the entropy, the more complex and random the sequence; the lower the entropy, the sequence is more regular and more close to the deterministic signal, so it is easier to predict.

2.2. The basic-scale entropy of typical signal

We analyse the basic-scale entropy of typical signals to verify its applicability and effectiveness. Figure 1 shows the base-scale entropy under the different data points of several typical signals. The production conditions of the typical signals are as follows:

(1) Sinusoidal signal: $y = \sin\left(\frac{2\pi}{600}x\right)$.

(2) Lorenz chaotic system: $\left\{\begin{array}{l} \frac{dx}{dt} = 16(y-x) \\ \frac{dy}{dt} = (45.92x - y - xz) \\ \frac{dz}{dt} = (xy - 4z) \end{array}\right\}$, and the initial condition is $\left\{\begin{array}{l} x_0 = -1 \\ y_0 = 0 \\ z_0 = 1 \end{array}\right\}$. In this paper we analyse the data points in the x-direction.

(3) The Chen chaotic system is described as $\left\{\begin{array}{l} \frac{dx}{dt} = a(y-x) \\ \frac{dy}{dt} = (c-a)x - xz + cy \\ \frac{dz}{dt} = xy - bz \end{array}\right.$, where $a = 35$, $b = 3$, $c = 28$, and the initial point is $(-1, 0, 1)$.

(4) Henon mapping: $\begin{cases} x(n+1) = 1 - a * x(n)^2 + y(n) \\ y(n+1) = b * x(n) \end{cases}$ when $a = 1.4$, $b = 0.3$, $x_0 = y_0 = 0.4$, the system is a chaotic system.

(5) Gaussian noise: it is a group of pseudo-random numbers, which is produced by the WGN function in MATLAB.

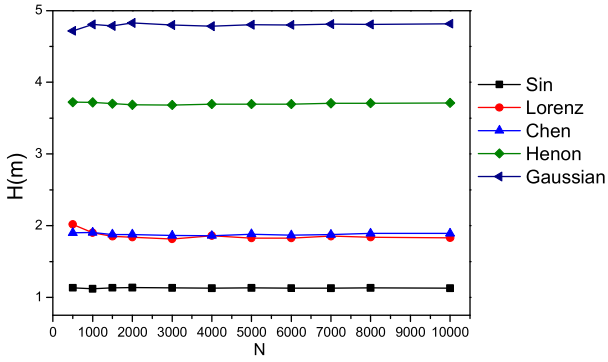

Figure 1. The base-scale entropy under the different data points of several typical signals.

As can be seen in Figure 1, the data length has little effect on the basic-scale entropy of typical signals. Therefore, when calculating the basic-scale entropy values, we can select fewer points, which can improve the computing speed. In addition, the Gaussian noise has a maximum base-scale entropy value, which means that the Gaussian noise is more complex and random. The base-scale entropy values of the sinusoidal signal are minimum, which illustrates that the sinusoidal signal has periodic properties. The base-scale entropy values of the Henon mapping are a bit lower than those of the Gaussian noise, which shows that the Henon mapping signal also has the higher complexity. Moreover, the Lorenz chaotic system and the Chen chaotic system have the similarity distributions of base-scale entropy values; therefore, they have the similar complexity. The results show that the base-scale entropy method can discriminate the different typical signals and can be used to analyse the complexity of time series. Moreover, it also can be used to study the deterministic of complex sequences.

3. Root mean square (RMS)

Different signals have different energies, and the value of energy can also reflect the characteristics of the signal. For the gas–liquid two-phase flow, the information of different flow patterns has different energy due to the acquisition manners. Therefore, the two-phase flow can be characterized from the energy point of view. In this paper, the energy value of the signal is extracted, and it is used as a characteristic parameter to identify and distinguish the two-phase flow.

There are many methods for extracting energy characteristics, and the root mean square (RMS) value (Wu et al., 2013) is a traditional and simple method to measure the signal's energy statistically. The RMS value represents the different characteristics of the signal. The higher RMS value of the signal shows that its energy is stronger and it is more periodic, while the lower RMS value shows that its energy is weaker and it is more random. Therefore, the RMS energy method can be used as the index for analysing the characteristics of gas–liquid two-phase flow patterns.

For a random sequence $x = \{x_i, i = 1, 2, \ldots, N\}$, its RMS is defined as

$$x_{\mathrm{RMS}} = \sqrt{\frac{1}{N}\sum_{i=1}^{N} x_i^2} = \sqrt{\frac{x_1^2 + x_2^2 + \ldots + x_N^2}{N}} \tag{6}$$

where N is the number of data points for the sequence.

4. Analysis of the characteristics of two-phase flow pattern

In this paper, we aim to study a type of simple and quick analysis method to identify flow regimes of the gas–liquid two-phase flow. Because the base-scale entropy needs less data and calculates quickly and the RMS method is a simple energy analysis method, we extract the features of the bubble flow, the slug flow and the churn flow by using these two methods, and then we characterize the complexity of the gas–liquid two-phase flow by the two features. The acquisition process of conductance fluctuating signals of three typical flow patterns refers to Zhai & Jin, 2016. The conductance fluctuating signals of the three typical flow patterns under the different gas flow rate conditions are shown in Figure 2 when the water flow rate is 8 m^3/h, where Q_w is the flow rate of liquid phase (m^3/h) and Q_g is the flow rate of gas phase (m^3/h).

The bubble flow usually occurs in the lower speed case of the gas stream, the trajectory of air bubble is random and complex, it rises with the liquid flow in the tube, and the signal is similar to the random signal. As we can see, the fluctuating signals of the bubble flow are rather random and can be characterized with very low amplitude. With the increase of gas velocity, the gas plugs and liquid plugs change regularly. Due to the destabilization of the liquid flow, the conductance fluctuating signals of the two-phase flow have the intermittent peak value and high amplitude. As to the churn flow, when the gas plugs and liquid plugs rise in the tube, because of the gravity, the liquid plugs fall down and collide with the incoming flows of the next moment. It vibrates alternately upward and downward in the pipe, exhibiting the irregularity and chaotic characteristics of conductance signals, which are similar to bubble flow patterns. However, the churn flow has the higher amplitude and weaker randomness than the bubble flow.

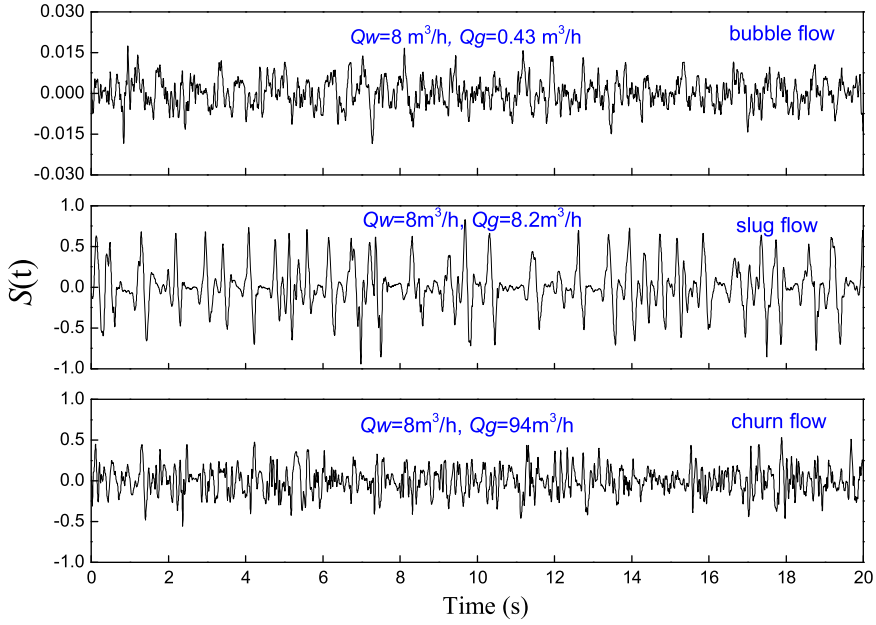

Figure 2. Conductance fluctuating signals of three typical flow patterns when $Q_w = 8\,m^3/h$.

4.1. The BE analysis of two-phase flow pattern

In this paper we research the base-scale entropy of conductance fluctuating signals of three typical flow patterns, and choose $m = 4, \alpha = 0.2, N = 500$ referring to (Zhai & Jin, 2016). Figure 3 depicts the base-scale entropy distribution with liquid flow rates including 1, 2, 4, 6, 8, 12 m^3/h and gas flow rates change from 0.2 to 140 m^3/h. From the base-scale entropy distribution shown in Figure 3, the slug flow has the smaller base-scale entropy values, which range from 2.67 to 2.83, and those of the churn flow range from 2.80 to 2.97. But the bubble flow has the larger base-scale entropy values and they lie between 2.93 and 3.05. The results suggest that the motions of the bubble flow and the churn flow

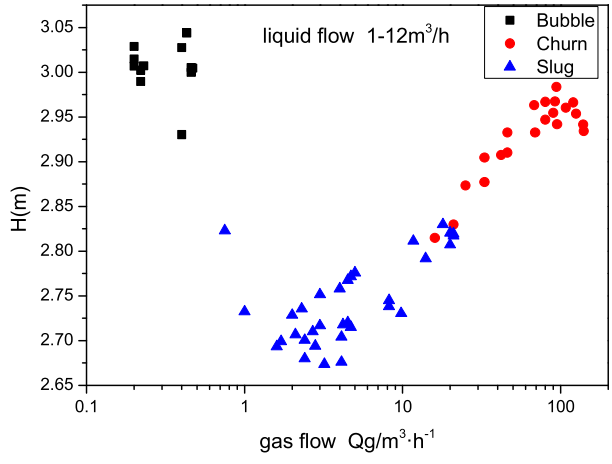

Figure 3. Base-scale entropy distribution of the gas–liquid two-phase flow.

are random; however, randomness of the churn flow is weaker than that of the bubble flow. As to the slug flow, it presents deterministic features and it has lower complexity. The BE, as the feature of the characterization of the gas–liquid two-phase flow, can distinguish the different flow patterns. In the BE analysis there are two points partly overlapped between the churn flow and the slug flow due to the measured process. The overlapping points should be the flow transition phase by the analysis.

In order to analyse the changes of complexity better under different gas–liquid two-phase flow conditions, distribution graphs of base-scale entropy were obtained when the water flow was 2, 4, 6, 8, 12 m^3/h as shown in Figure 4.

Figure 4 shows that with the increase of the gas flow rate, the base-scale entropy values become smaller when the bubble flow is transformed to the slug flow, this shows that the certainty of the two-phase flow system is enhanced. When the slug flow is transformed to the churn flow, the base-scale entropy values become larger, this shows that the motion behaviour of the two-phase flow system becomes random. Moreover, the base-scale entropy of the bubble flow is larger than that of the churn flow, which is also consistent with the previous analysis.

4.2. The RMS analysis of two-phase flow pattern

The RMS is the simple energy analysis method of extracting feature and is used to have a complement with the BE in this paper. The RMS values represent the energy distribution of signals. The RMS values of conductance fluctuating signals of three typical flow patterns are shown in

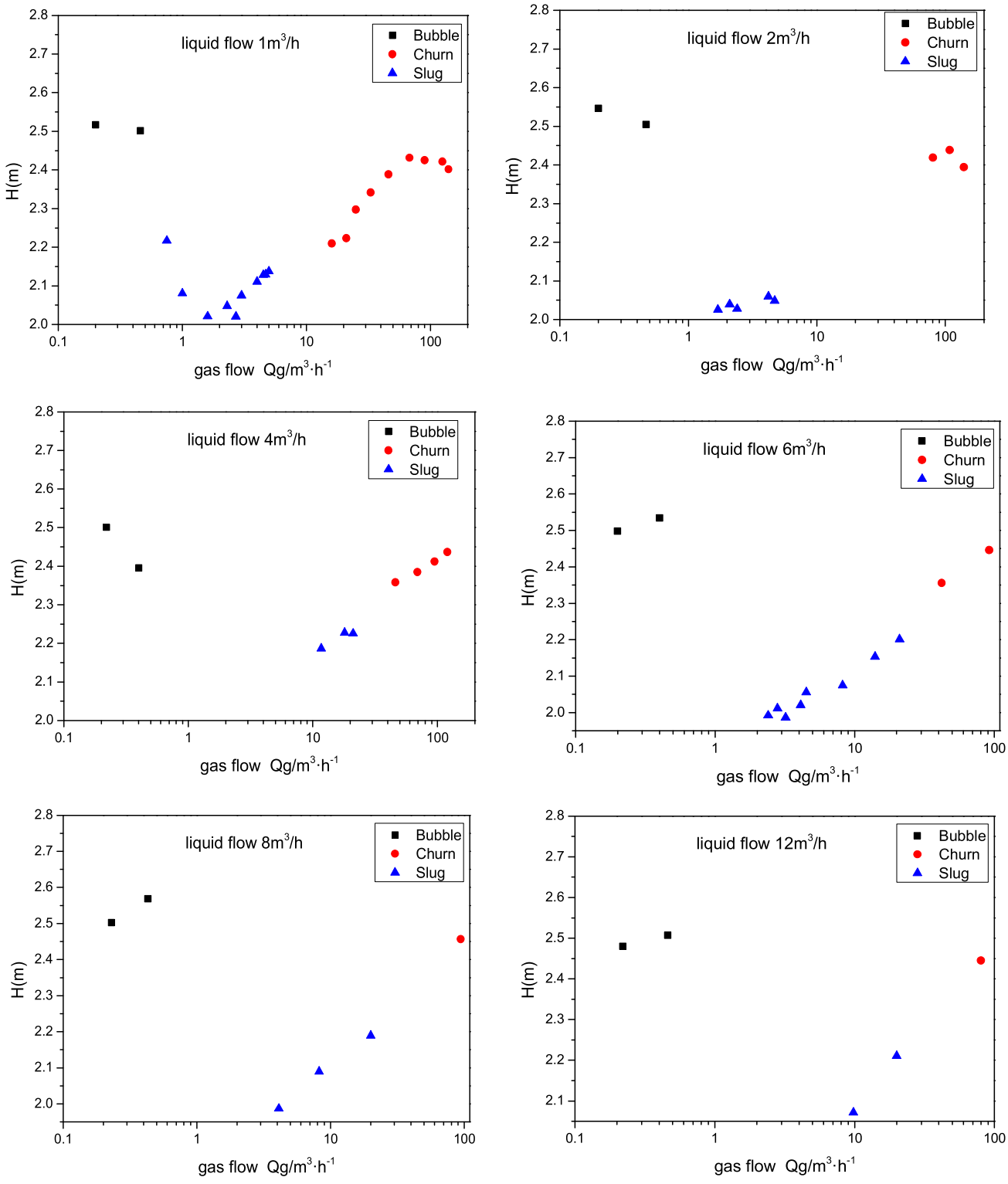

Figure 4. Base-scale entropy distribution under different gas-phase flow conditions.

Figure 5. From Figure 5, we can see that the slug flow has the largest RMS values, which shows that the energy of the slug flow is strongest and it is more periodic. While the RMS values of the churn flow and the bubble flow are smaller, which indicate that their energy is weaker and their motions are random; however, randomness of the churn flow is weaker than that of the bubble flow. Consequently, the RMS can also be regarded as a feature to analyse the characteristics of the gas–liquid two-phase flow, and it can identify the flow patterns. Similarly, in the RMS analysis there are the same overlapped points as the BE analysis due to the measured process. Next, the

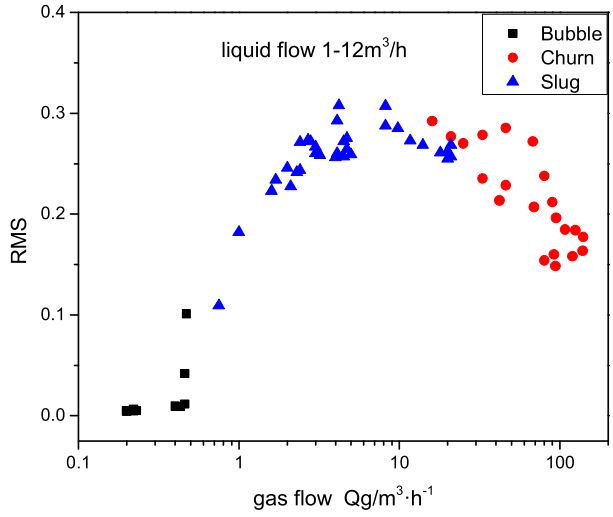

Figure 5. RMS distribution of the gas–liquid two-phase flow.

distribution graphs of the RMS were obtained when the water flow were 1, 2, 4, 6, 8, 12 m^3/h as shown in Figure 6.

Figure 6 shows that with the increase of the gas flow rate, the RMS values become larger when the bubble flow transforms to the slug flow, which shows the certainty of the two-phase flow system is enhanced. While the slug flow transforms to the churn flow, the RMS values become smaller which indicates the motion behaviour of the two-phase flow system becomes random.

5. Separability measure analysis of the extracted features

In order to verify the effectiveness of the extracted features, we analyse the separability measure of the BE and the RMS.

The feature set $A = \{a_i, i = 1,2,\ldots,k_a\}$ is constituted by the same characteristics of the signal. The within-class distance is one of the important indices to measure the mode separability (Zhou, Sun, & Li, 2010). The square of the within-class distance is defined as the root mean square value of distance of feature vectors in the set:

$$L^2(\{a_i\},\{a_j\}) = \frac{1}{k_a(k_a-1)}\sum_{i=1}^{k_a}\sum_{j=1}^{k_a} d^2(a_i,a_j) \qquad (7)$$

where $d^2(a_i,a_j) = (a_i - a_j)^2, i = j = 1,2,\cdots k_a$.

For the features sets $A = \{a_i, i = 1,2,\cdots,k_a\}$ and $B = \{b_j, j = 1,2,\cdots,k_b\}$, the square of the between-class distance is defined as

$$L^2(\{a_i\},\{b_j\}) = \frac{1}{k_a k_b}\sum_{i=1}^{k_a}\sum_{j=1}^{k_b} d^2(a_i,b_j) \qquad (8)$$

where $d^2(a_i,b_j) = (a_i - b_j)^2, i = 1,2,\cdots k_a; j = 1,2,\cdots k_b$.

If the approach of feature extraction makes the within-class distance smaller, and the distance between-class larger, then we can state that this approach of feature extraction is good. According to these two distances, separability measure $J_{A,B}$ is defined as

$$J_{A,B} = \frac{L^2(\{a_i\},\{b_j\})}{L^2(\{a_i\},\{a_i\}) + L^2(\{b_j\},\{b_j\})} \qquad (9)$$

where $L^2(\{a_i\},\{b_j\})$ is the square of the between-class distance of A and B, $L^2(\{a_i\},\{a_i\})$ and $L^2(\{b_j\},\{b_j\})$are the squares of the within-class distances of the feature sets A and B, respectively.

$J_{A,B}$ is an index to measure the separability between different classes. The separability between A and$B$ is better if $J_{A,B}$ is larger, while it is worse when $J_{A,B}$ is smaller.

The separability measures of the BE and the RMS are calculated, and the results are listed in Table 1.

From Table 1, it can be seen that the distance data (0.0016, 0.0059, 0.0041) and (0.0017, 0.0027, 0.0047) on the main diagonal line are the within-class distances of the same flow patterns for the BE and the RMS, respectively. The other distance data (0.0692, 0.0088, 0.0365) and (0.0581, 0.0420, 0.0051) are the between-class distances of different flow patterns for the BE and the RMS, respectively. The separability measure $J_{A,B}$ has the same distribution except for the main diagonal line.

According to the data in Table 1, we know that the between-class distance of the bubble flow and the churn flow for the BE is 0.0088, it is close to the within-class distances of the bubble flow (0.0016) and the churn flow (0.0041), which shows that the bubble flow and the churn flow are very similar. However, the between-class distance of the bubble flow and the churn flow for the RMS is 0.0420, it is far larger than the within-class distance of the bubble flow (0.0017) and the churn flow (0.0047), which indicates that the RMS is better than the BE in the distinguishing effects of the bubble flow and the churn flow. In addition, we can see that the separability measure $J_{A,B}$ of the bubble flow and the churn flow for the BE is 1.5439, while the $J_{A,B}$ of the bubble flow and the churn flow for the RMS is 6.5625, which also shows that the RMS is better than the BE in the distinguishing effects of the bubble flow and the churn flow. For the bubble flow and the slug flow, the between-class distance for the BE is 0.0692, and the between-class distance for the RMS is 0.0581. These between-class distances are larger than the within-class distances of the bubble flow (0.0016, 0.0017) and the slug flow (0.0059, 0.0027). Moreover, the $J_{A,B}$ of the BE for the bubble flow and the slug flow is 9.2267, while that of the RMS is 13.2045, which indicates that the BE and the RMS methods can distinguish the bubble flow and the slug flow clearly, and the RMS method is superior to the BE method. As to the churn flow and the slug flow, the

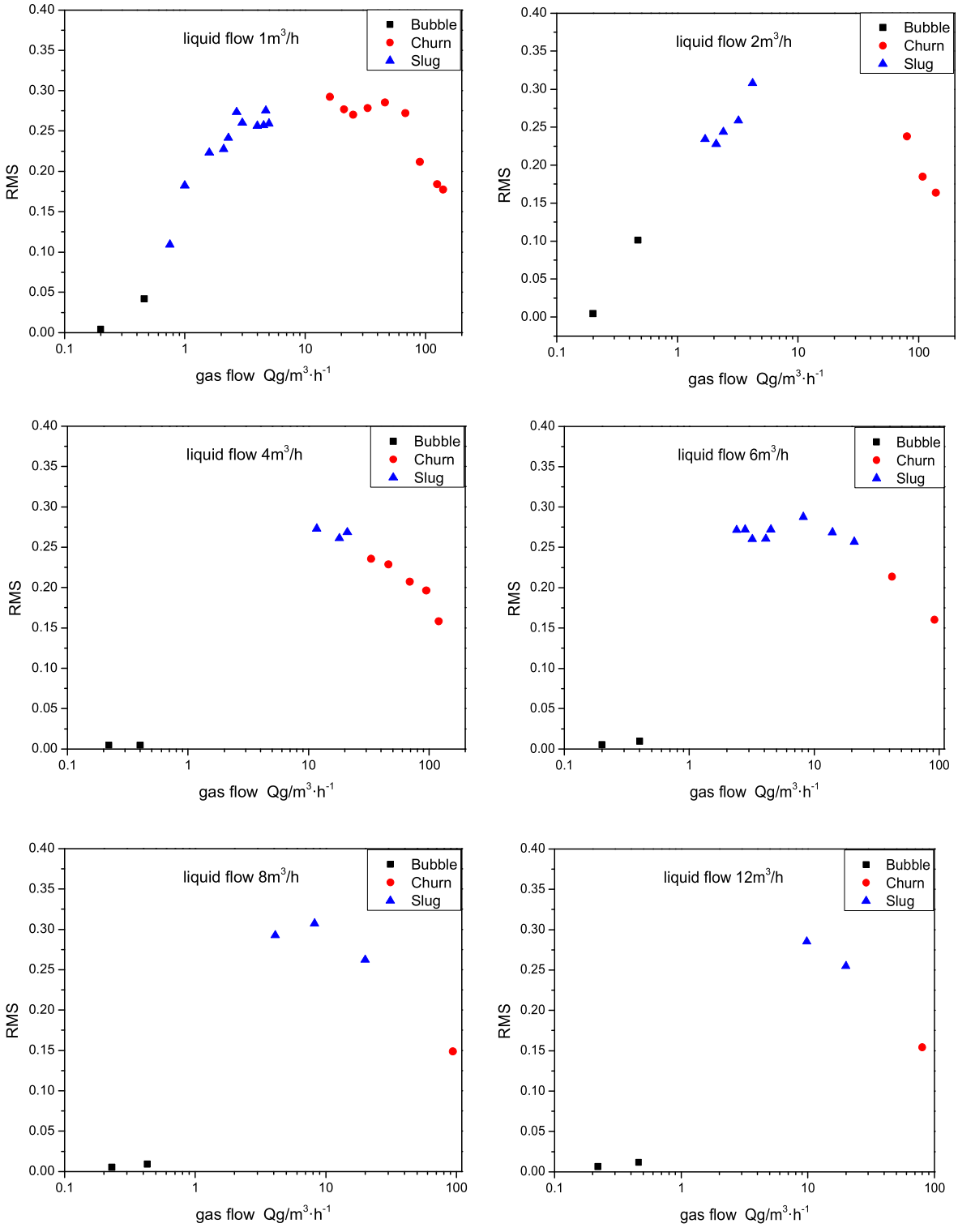

Figure 6. RMS distribution under different gas-phase flow conditions.

between-class distance for the BE is 0.0365, and it is far bigger than the between-class distance (0.0051) for the RMS. In addition, the $J_{A,B}$ (3.6500) of the BE for the churn flow and the slug flow is also far larger than that of RMS (0.6892). The above analysis shows that the BE is better than the RMS in the identification of the churn flow and the slug flow. All the above analysis states that the BE and the RMS energy method can identify the flow patterns and complement each other when discriminating the bubble flow and the slug flow, the churn flow and the slug flow. Moreover, the analysis results are consistent with the information given in Figures 3 and 5.

Table 1. Comparison of measurement feasibility between BE and RMS.

		Distance			$J_{A,B}$		
Feature	Flow pattern	Bubble	Slug	Churn	Bubble	Slug	Churn
BE	Bubble	0.0016	0.0692	0.0088	0	9.2267	1.5439
	Slug	0.0692	0.0059	0.0365	9.2267	0	3.6500
	Churn	0.0088	0.0365	0.0041	1.5439	3.6500	0
RMS	Bubble	0.0017	0.0581	0.0420	0	13.2045	6.5625
	Slug	0.0581	0.0027	0.0051	13.2045	0	0.6892
	Churn	0.0420	0.0051	0.0047	6.5625	0.6892	0

6. Conclusions

Considering the conductance fluctuating signals of the gas–liquid two-phase flow have nonlinear and nonstationary properties, we present a simple and quick strategy, which combines the BE method and RMS energy method, to extract the features of the gas–liquid two-phase flow, and to characterize the complexity of the gas–liquid two-phase flow patterns. We employ the separability measure to verify the effectiveness of the extracted features. The results show that the proposed strategy can identify different flow patterns, and the RMS method is superior to the BE method between the bubble flow and the slug flow in the distinction effect, while for the churn flow and the slug flow, the BE method is better than the RMS method. According to the analysis, we know that the combined strategy presented in this paper can not only distinguish the different flow patterns quickly but also complement each other. This paper provides a simple strategy to identify the flow patterns of the two-phase flow and new vision on the flow pattern characteristics analysis of the gas–liquid two-phase flow.

Disclosure statement

No potential conflict of interest was reported by the authors.

Funding

This project supported by the Taishan Scholar Project Fund of Shandong Province of China; National Natural Science Foundation of China [61472195, 61773227].

References

Fan, C. L., Haojie, L., & Yinghui, S. (2015). Characterization of two-phase flow pattern based on multi-scale base-scale entropy. *Journal of Qingdao University of Science and Technology (Natural Science Edition)*, *36*(6), 680–684.

Fan, C. L., Jin, N. D., Chen, X. T., Dou, F. X., & Gao, Z. K. (2015). Two-phase flow structure in multi-scale complexity entropy causality plane. *CIESC Journal*, *66*(4), 1301–1309.

Göksu, H. (2018). BCI oriented EEG analysis using log energy entropy of wavelet packets. *Biomedical Signal Processing and Control*, *44*, 101–109.

Hu, J. F., Mu, Z. D., & Xiao, D. (2008). Classification of motor imagery EEG signals based on energy entropy. *Computer Engineering and Applications*, *44*(33), 235–238.

Li, H. Q. (1991). *Parameter detection and application of two-phase flow* (pp. 1–8). Zhejiang: Zhejiang University Publishing House.

Li, J. M., Li, M., & Zhang, J. F. (2017). Rolling bearing fault diagnosis based on time-delayed feedback monostable stochastic resonance and adaptive minimum entropy deconvolution. *Journal of Sound and Vibration*, *401*, 139–151.

Li, J., & Liu, D. Z. (2012). Changes of entropy and power spectrum in circadian rhythm for heart rate variability signals. *Acta Physica Sinica*, *61*(20), 547–552.

Li, H. W., Zhou, Y. L., Ren, S. L., & Yang, Y. (2012). Application of conductance signals analysis of gas-liquid two-phase flow patterns based on symbolic dynamics entropy. *Journal of Chemical Industry and Engineering*, *63*(11), 3486–3492.

Liu, Z. L., & Shang, P. J. (2018). Generalized information entropy analysis of financial time series. *Physica A: Statistical Mechanics and its Applications*, *505*, 1170–1185.

Liu, T. B., Yao, W. P., Ning, X. B., Ni, H. J., & Wang, J. (2013). The base scale entropy analysis of f MRI. *Acta Physica Sinica*, *21*(62), 218704.

Tan, C., & Dong, F. (2013). Parameters measurement for multiphase flow process. *Acta Automatica Sinica*, *39*(11), 1923–1932.

Wu, S. D., Wu, C. W., Wu, T. Y., & Wang, C. C. (2013). Multi-scale analysis based ball bearing defect diagnostics using mahalanobis distance and support vector machine. *Entropy*, *15*, 416–433.

Yan, B. G., & Zhao, T. T. (2011). Multiscale base-scale entropy analysis of heart rate variability signal. *Acta Physica Sinica*, *60*(7), 822–826.

Zhai, L. S., & Jin, N. D. (2016). Multi-scale cross-correlation characteristics of void fraction wave propagation for gas-liquid two-phase flows in small diameter pipe. *Acta Physica Sinica*, *1*(65), 010501.

Zhou, Y. L., Sun, B., & Li, H. W. (2010). *Parameter detection theory and application of multi-phase flow* (pp. 68–70). Beijing: Science Publishing House.

Zhou, Y. L., Yin, H. M., & Ding, H. X. (2016). Application of multi-scale entropy in analyzing pressure difference signals of gas-liquid two-phase flow in rod bundled channel. *CIESC Journal*, *67*(9), 3625–3632.